Encoding Information on the Excited State of a Molecular Spin Chain

Kostantine Katcko, Etienne Urbain, Franck Ngassam, Lalit Kandpal, Bhavishya Chowrira, Filip Schleicher, Ufuk Halisdemir, Di Wang, Torsten Scherer, Damien Mertz, et al.

DOI: 10.1002/10.1002/adfm.202009467
This is the submitted version of a manuscript that was published in Adv. Func. Mater. in 2021 at the above DOI.

Encoding information on the excited state of a molecular spin chain

K. Katcko[1]*, E. Urbain[1]*, F. Ngassam[1]*, L. Kandpal[1], B. Chowrira[1,2], F. Schleicher[1], U. Halisdemir[1], D. Wang[3], T. Scherer[3], D. Mertz[1], B. Leconte[1], N. Beyer[1], D. Spor[1], P. Panissod[1], A. Boulard[1], J. Arabski[1], C. Kieber[1], E. Sternitzky[1], V. Da Costa[1], M. Hehn[4], F. Montaigne[4], A. Bahouka[5], W. Weber[1], E. Beaurepaire[1†], C. Kübel[3,6], D. Lacour[4], M. Alouani[1], S. Boukari[1], M. Bowen[1@]

[1] *Institut de Physique et Chimie des Matériaux de Strasbourg, UMR 7504 CNRS, Université de Strasbourg, 23 Rue du Læss, BP 43, 67034 Strasbourg, France.*

[2] *Synchrotron SOLEIL, L'Orme des Merisiers, Saint-Aubin, BP 48, 91192 Gif-sur-Yvette, France*

[3] *Institute of Nanotechnology, Karlsruhe Institute of Technology, Hermann-von-Helmholtz Platz 1, 76344 Eggenstein-Leopoldshafen, Germany*

[4] *Institut Jean Lamour UMR 7198 CNRS, Université de Lorraine, BP 70239, 54506 Vandœuvre les Nancy, France.*

[5] *IREPA LASER, Institut Carnot MICA, Parc d'innovation - Pole API, 67400 Illkirch, France*

[6] *Joint Research Laboratory Nanomaterials, Technical University Darmstadt, Department of Materials & Earth Sciences, Alarich-Weiss-Straße 2, 64287 Darmstadt, Germany*

* These authors contributed equally.
† Deceased April 24th, 2018.
@ e-mail: bowen@unistra.fr

Keywords: spintronics, spin chain, information encoding, quantum technology, magnetic anisotropy

Abstract:

The quantum states of nano-objects can drive electrical transport properties across lateral [1–6] and local-probe [7–13] junctions. This raises the prospect of encoding information at the quantum level using the electrical generation of spin-flip excitations between electron spins [7–13]. However, this electronic state has no defined magnetic orientation, and is short-lived [14]. We overcome these limitations and experimentally demonstrate this steady-state capability in solid-state spintronic devices. We observe that the excited quantum state of a spin chain formed by Co phthalocyanine molecules coupled [15] to a ferromagnetic electrode constitutes a distinct

magnetic unit endowed with a coercive field. This generates a specific steady-state magnetoresistance (MR) trace that is tied to the spin-flip conductance channel, and is opposite in sign to the ground state MR term, as expected from spin excitation transition rules. The experimental 5.9meV thermal energy barrier between the ground and excited spin states is confirmed by density functional theory, in line with a phenomenological theory of macrospin transport that reproduces our experimental results. This low-voltage control over a spin chain's quantum state and spintronic contribution lays a path for transmitting spin wave-encoded information across molecular layers [16]. It should also stimulate quantum prospects for the antiferromagnetic spintronics and oxides electronics communities [17].

Main Text

Inelastic excitations can cause a large increase in the current flowing across a set of coupled electron spins by inducing electronic transitions in the spin chain from its quantum ground state to an excited state. Due to the conservation of spin angular momentum and transition rules [14], this spin-flip process causes minority spin states from the electrode to transport as majority states. The converse scenario is forbidden. The spin polarization of the spin excitation current is indirectly seen in scanning tunnelling spectroscopy experiments by comparing the amplitudes of the resulting conductance peaks upon reversing the bias voltage. Here, the magnetic orientation isn't set, but can be influenced by a local [8,9,13] or external [18,19] magnetic field. Furthermore, since the excited states of a spin chain are dynamical, they are expected to be short-lived, before spin angular momentum transfer to the transport electron causes the chain to return to its ground state [14].

Solid-state spintronic devices typically detect the spin polarization of electrical currents by studying how the current amplitude changes upon flipping the magnetization of the device's

ferromagnetic (FM) electrodes. This effect is called magnetoresistance (MR), and constitutes the technological basis for encoding and transmitting information using the electron spin [20]. Spin-polarized transport across a device's metallic/semiconducting antiferromagnetic layer can promote macroscale effects, from tunneling anisotropic magnetoresistance [21] and interface charging [22,23] to the manipulation of AF domains [24,25]. Moving from the macroscale to the AF spin chain's quantum properties, indirect evidence suggests that MR might be used in a solid-state device to detect changes in the AF spin chain's quantum state [26,27].

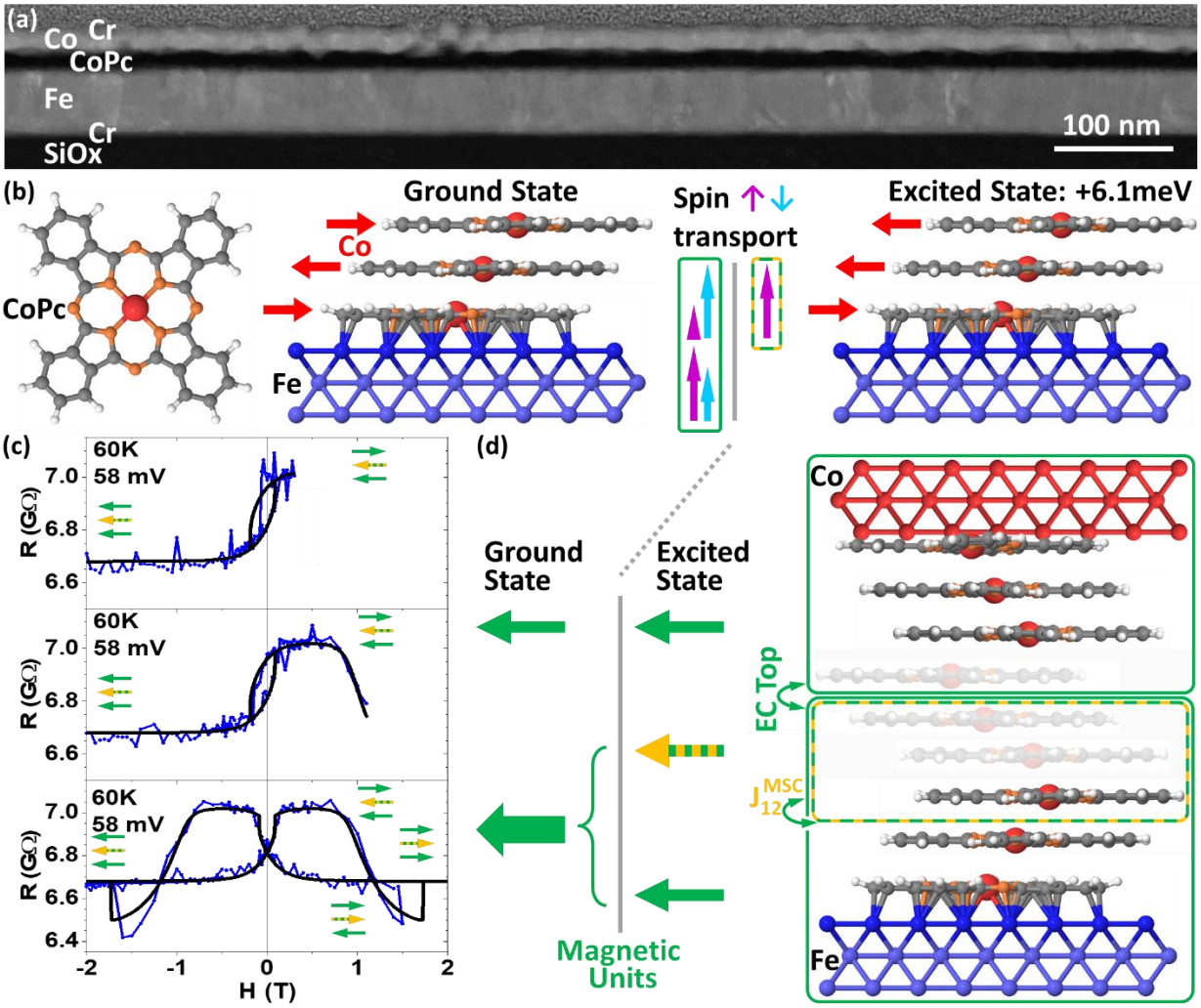

Figure 1: Spin-flip magnetoresistance. *(a) Cross-sectional TEM image of the stack. (b) CoPc molecular spin chain atop a Fe electrode. Spin-polarized transport across the spinterface and the molecular spin chain in its ground and excited states. The latter state promotes additional spin ↑ transport, which can be analyzed using a FM top electrode (not shown). (c) Major and minor R(H) loops (blue data) at T=60K and V=58mV reveal three R levels due to the magnetization reversal of three magnetic units (green/yellow arrows). (d) Schematic of the two*

main magnetic units involving the FM electrodes (green boxes). The lower magnetic unit (large green arrow) includes an electrically driven 3rd unit (green/yellow box and arrow) due to spin excitations along the MSC. Not all molecular layers are shown (semi-transparent zone). The macrospin model's coupling terms ECTop and J_{12}^{MSC} *between the central and outer units are shown. See text for details, and fitting parameters in Suppl. Note 1. R(H) fits (black lines in panel c) using* K_t/M_t *=0.26T,* θ_{Mt}*=60º,* K_b/M_b *=4.95T,* θ_{Mb}*=-4º, ECTop=-0.05T,* J_{12}^{MSC} *=1.28T,* R_0*=6.68GΩ, MRTop=-2.4% and SpinFlipMR=5.1%.*

To encode information in a technologically relevant way, the excited quantum state of a molecular spin chain should thus exhibit a magnetic steady state that can be manipulated independently. Noting that a FM can set the spin referential of a molecular spin chain (MSC) [15], we begin by sandwiching a thin film of antiferromagnetic spin chains formed by Co phthalocyanine molecules with S=1/2 [7,28] between FM metallic thin films acting as injector/analyzer of the current's spin polarization. Here, the antiferromagnetic molecular layer is the device's active spintronic spacer, rather than an adjunct layer to magnetically pin a FM electrode through the exchange bias effect as is commonplace in spintronic devices [29].

Figure 1(a) shows a cross-sectional transmission electron microscopy (TEM) image of our entire *in-situ* grown FM/molecular layer/FM stacks. Despite the presence of some structural imperfections, the wide field-of-view image confirms the continuity of our layered heterostructure. Figure 1(b) depicts the CoPc molecule and spin-polarized transport proceeding from our devices' lower Fe electrode across the MSC. The spin polarization P of the current changes sign [30] when flowing from the FM metal onto the FM/molecule interface, i.e. the 'spinterface' [31], and the amplitude of P becomes large. In the case of the Fe/CoPc spinterface, P<0 [30]. This P<0 current [30] that thereafter flows across the MSC in its ground state is expected to be supplemented by a current across the MSC's excited state with a P>0 [7–9,12,27].

Our junctions are crafted from entire *in-situ* grown FM/molecular layer/FM stacks, thereby preserving nominal structural/magnetic properties, especially at interfaces, using a novel, solvent-and resist-free processing technique inspired by nanosphere lithography [32]. This novel technique is described in Supplementary Note 4, and was implemented using 500nm-diameter SiO_2 nanobeads. Since intrachain magnetic interactions dominate the very weak interchain interactions in Pc thin films [28], and since transport in dielectric devices proceeds along a nanoscale path [33,34], it is possible to observe quantum transport effects due to the MSC in a solid-state mesoscopic device that are similar to those observed in STM-assembled model junctions [2,2,7–14]. Naturally, a solid-state approach cannot straightforwardly reveal a MSC's details (length, geometry…), but it endows fundamental quantum transport effects with technological relevance, and enables their study while varying the applied magnetic field, and over a wide temperature range. The following dataset, which is typical of results found on several junctions (see Methods), was entirely acquired on a Fe/CoPc(20nm)/Co junction with resistances R(300K)=32kΩ and R(17K)=11GΩ at 20mV. This underscores thermally activated hopping transport [35,36] across the thin CoPc layer.

We first examine magnetotransport at 60K. Fig. 1c shows *R(H)* loops at 58mV following a cooldown at H=-1T. As the positive maximum H is increased, one notices a 1st resistance jump near H=0, and a 2nd resistance change centered around H=1.17T that is reversible as long as the resistance baseline at H=-2T isn't exceeded. For higher positive field sweeps, a third resistance change is observed and the *R(H)* loop becomes field-symmetric.

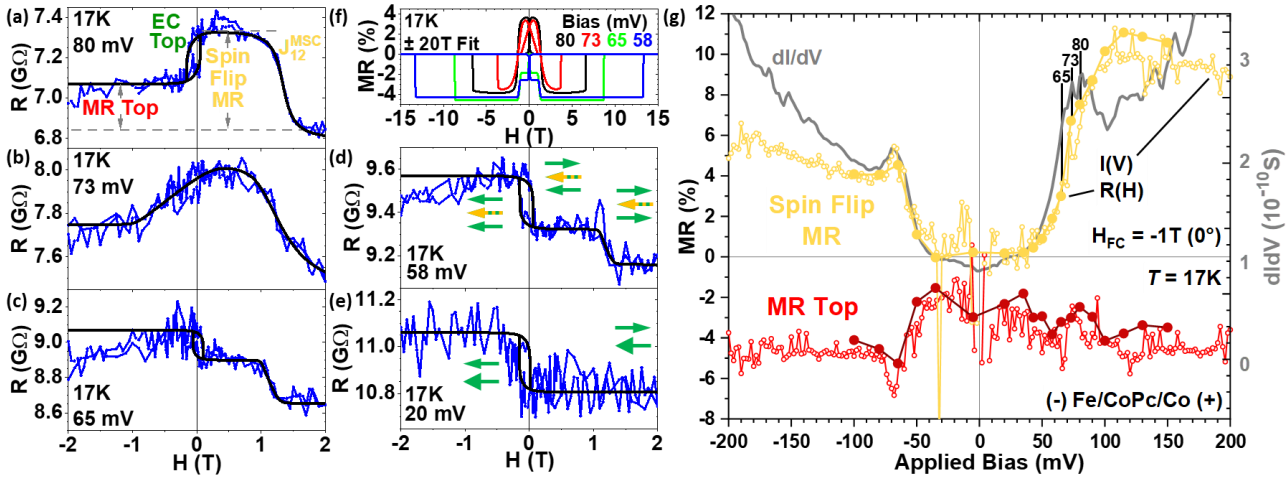

Figure 2: Electrical onset of spin-flip magnetoresistance. *(a-e) Experimental (blue) R(H) loops at 17K for 20 < V(mV) < 80 and associated fits (black), also represented in panel f for ±20T. The red/green arrows refer to the magnetic units. The larger green arrow in panel e represents both lower units in the absence of spin excitations (see Fig. 1d). (g) Bias dependence of dI/dV, and of MRTop / SpinFlipMR inferred from I(V) and R(H) data. SpinFlipMR tracks dI/dV and generates a specific R(H) trace. See text for details, and fitting parameters in Suppl. Note 1.*

The three resistance levels observed correspond to three magnetic configurations, symbolized by green/red arrows in Fig. 1d, of three magnetic units. To better understand their origin, we now examine magnetotransport at 17K, starting with the R(H) loops within 20 < V(mV) < 80mV (Fig. 2(a-e)). Going from T=60K to T=17K causes the R(H) loop at 58mV to no longer be symmetric: the final reversal occurs for |H|>2T. We experimentally define *MRTop*=*R*(2T)/*R*(-2T)-1 and *SpinFlipMR*= *R*(H_f)/*R*(2T)-1 (H_f = 1T for 17 < *T*(K) < 50, H_f< 1T for *T* > 50K, see Fig. 3), and schematize these MR contributions in the *R(H)* at 80mV and *T*=17K (see Fig. 2a)[1]. At 17K, reducing V causes *SpinFlipMR* to decrease, and disappear for V=20mV (only two *R* plateaus appear in Fig. 2e). Similar effects are observed for *V*<0 (data not shown).

[1] Due to our experimental limitation |H|<2T, when comparing the model with experiment, we approximate $R_0 = R(-2T)$. Small deviations between experimental and modelled values of *MRTop* and *SpinFlipMR* can occur because full magnetization reversal of the bottom magnetic unit can be incomplete within |*H*|<2T. Nevertheless, dataset consistency criteria and the shape of the R(H) data strongly limit possible errors. See Suppl. Note 1 for details.

The bias dependence of *dI/dV* (gray line of Fig. 2g) reveals a mostly constant amplitude for $|V|<35$mV, and large increases for $|V|>35$mV, punctuated by peaks at $|V|\approx 70$mV. The *dI/dV* amplitude further increases at higher bias. In line with previous literature [7,8,27] on STM-assembled and solid-state-based transport across spin chains, we interpret these *dI/dV* features as the signature of spin excitations[2].

We observe that *SpinFlipMR* spectroscopically tracks the *dI/dV* conductance increase, both from *R(H)* and *I(V)* data (see Fig. 2g).[3] To the best of our knowledge, this is the first observation of a specific MR signal that is driven to appear due to bias voltage, and whose amplitude tracks a conductance increase. Given the above interpretation of *dI/dV*, we conclude that *SpinFlipMR* arises from the opening of spin-flip channels of transport across MSCs. The opposite sign of P of this spin-flip transport channel compared to the ground-state transport channel is manifest in the opposite signs of *MRTop* and *SpinFlipMR*.

[2] The complicated bias drop due to hopping transport across the nominal 20 nm-thick CoPc junction could explain the higher bias onset compared to STM studies [7] and impedes a discussion on the effective MSC. This could also account for the different amplitudes in the *dI/dV* peaks for $V>0$ and $V<0$, alongside a spin-polarized transport explanation [8].

[3] The small voltage lag originates from spectroscopic averaging effects for current compared to conductance [37].

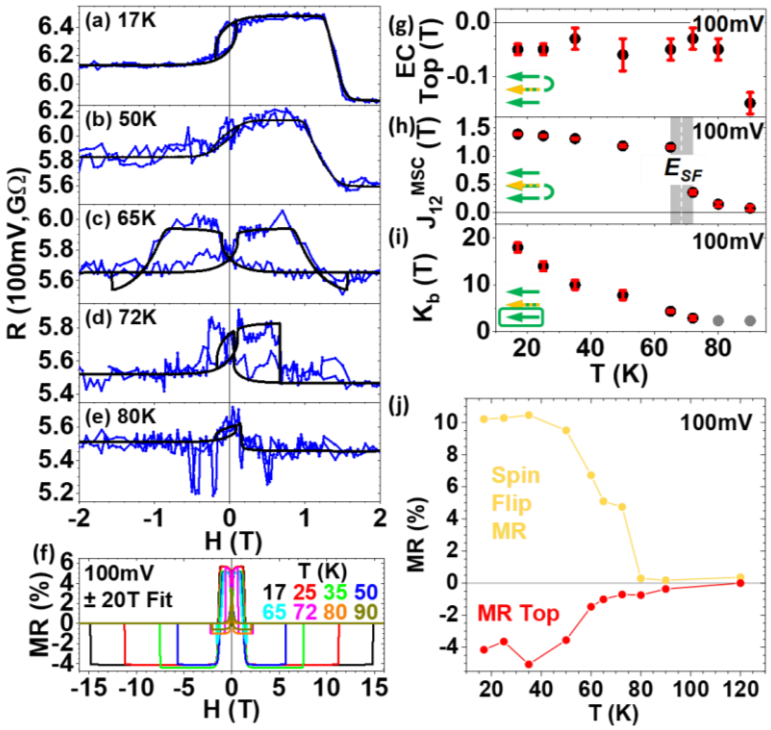

Figure 3: Thermal stability of spin-flip magnetoresistance. *(a-e) R(H) loops at 100mV for 17 < T(K) < 80. Data are in blue, while the modelled fits are in black and are also shown in panel f for ±20T. Temperature dependencies of (g) ECTop, (h) J_{12}^{MSC}, (i) K_b and (j) of SpinFlipMR and MRTop. The gray data in panel i for T≥80K are the minimum values required to obtain R(-2T)≠R(2T). The error bars for data in panels g-i are discussed in Suppl. Note 1.*

If electrically exciting the MSC only opened a conductance channel with opposite P, then the MR in Fig. 2e would eventually switch signs, but the shape of the R(H) would remain identical. The presence of the resistance change at H=+1.2T only when a spin excitation current is present (compare Fig. 2(d-e)) is surprising. This indicates that the magnetic unit responsible for *SpinFlipMR* is not only electrically driven, but is endowed with its own coercive field.

To study its energetics, we varied the temperature. We plot in Fig. 3(a-e) R(H) data at 100mV for 17 < T(K) < 80K. For 17 < T(K) < 55, the same flipping of the top and bottom magnetic units is observed for $|H| \leq 2$T (data at 55K not shown). For $60 \leq T(K) < 72$, a symmetric *R(H)* is observed (see also Fig. 1c). We witness a sharp change in the *H* dependence of the SpinFlipMR contribution at $T \approx 70$K, i.e. $E_{crit}=k_BT \approx 6$meV (compare Fig. 3a-c with Fig. 3d). For $T \geq 80$K, the *R(H)* loop has collapsed, and only low-field MR is observed until 100K.

To identify the corresponding scenario of spin excitation along the MSC, we utilized density functional theory (DFT; see Methods) and tested multiple scenario of molecular adsorption geometries and magnetization reversals (see Suppl. Note 3). We in particular calculated the energy cost of reversing the magnetization along the MSC. Note that, since the 1st CoPc molecule is chemisorbed onto Fe [7,38], the 1st CoPc molecule of the MSC is the 2nd CoPc ML atop Fe. We calculate an energy cost ΔE=6.1meV, i.e. $\Delta E \approx E_{crit}$, when the magnetization of the 3rd CoPc molecule is reversed relative to that of the 1st and 2nd CoPc MLs atop Fe (see Fig. 1b).

These experimental and theoretical results suggest that the magnetic coupling [15] between the FM electrode and the chain of paramagnetic centers accounts for the excited spin state acting as a distinct magnetic unit. Although the magnetic anisotropy of ground and excited spin states can in general differ [39], this outcome is surprising since the exchange bias at the spinterface is expected [30,40,41] to dominate. To confirm this point, we phenomenologically model magnetotransport involving three macrospins. The 'central' magnetic unit depicted by the red/green box in Fig. 1d comprises the portion of the MSC in the excited spin state. It is enclosed into a 'bottom' magnetic unit (green box) that also comprises the spinterface and Fe electrode. Its uniaxial anisotropy field K_b is therefore large due to several mechanisms of magnetic exchange bias at the spinterface [15,40]. This is confimed by field-cooling and angular studies (see Suppl. Note 2). The central and lower units are exchanged-coupled by J_{12}^{MSC}, such that we attribute a low anisotropy field K_c=5mT to the MSC in its excited state. [4] As we will see, the top magnetic unit is comprised of the Co layer directly coupled to a MSC, owing to a more diffuse interface. The presence in the nanotransport path of disjointed chains across the film

[4] Only at the (V=80mV,17K) and (V=100mV, 72K) critical points does K_c/M_c strongly increase, as expected in an exchange bias system near criticality [42]. See Suppl. Note 1 for details.

thickness is expected from both structural and magnetic studies [28,40], such that a weak AF exchange term *ECTop* is present between the top and central magnetic units.

To model our magnetotransport data, we first write the effective anisotropy field *K* of the nanotransport path across the top (i=t), central (i=c) and bottom (i=b) units as:

$$K = -\mu_0 \sum_{\boldsymbol{i=t,c,b}} \boldsymbol{H}.\boldsymbol{m_i} + \frac{1}{2}\sum_{\boldsymbol{i=t,c,b}} K_i \sin^2(\theta_{M_i} - \theta_{K_i}) - \sum_{\boldsymbol{i=t,c}} C_{bi}\, \boldsymbol{m_b}.\boldsymbol{m_i}.$$

where H is the applied magnetic field and, for each unit, m_i the reduced magnetization [5], θ_{M_i} the magnetization angle, and K_i its uniaxial anisotropy field with an easy axis angle θ_{K_i}. Finally, C_{bi} is the coupling strength between the bottom (b) and other (i=c,t) magnetic units. K, K_i and C_{ci} are expressed in Tesla. We define C_{bt} = *ECTop* and C_{bc}= J_{12}^{MSC}. For each H step, K is minimized to yield, for each magnetic unit, the magnetization's in-plane orientation. The resistance R due to non-collinear magnetizations M_t, M_b and M_c is:

$$R = R_0.\left[1 - \frac{MRTop}{2}\cdot(\mathbf{m_t}.\mathbf{m_b} - 1) - \frac{SpinFlipMR}{2}\cdot(\mathbf{m_t}.\mathbf{m_c} - \mathbf{1})\right].$$

MRTop is the MR due to flipping the magnetization of the top magnetic unit relative to that of harder magnetic units, i.e. to the bottom magnetic unit. *SpinFlipMR* considers the MR due to flipping both the top and central magnetic units (see Suppl. Note 1 for details on pairing magnetic units to MR terms).

Using this model, we can successfully fit all the unusual features (plateaus, reversals, coercive fields, loop shape, etc…) of our *R(H)* dataset in V,T parameter space (see black lines in Fig. 1c, Fig. 2a-e, Fig. 3a-e). We thus identify the sequential magnetization reversal of the three units (see corresponding green/red arrows, and *ECTop* and J_{12}^{MSC} labels in Fig. 2a). To illustrate the three reversals found at 60K (Fig. 1g) throughout the dataset, and since the third reversal can

[5] For simplicity, the magnetizations of two FM units are treated as identical, and are large compared to the magnetization of CoPc, which is neglected.

occur for $|H|>2$T, we also plot the *R(H)* phenomenology of the bias (Fig. 2f) and temperature (Fig. 3f) dependencies. The top magnetic unit's $K_t \approx 0.2$T is over an order of magnitude stronger than that of a free layer. We infer that it contains not only the top Co FM electrode, but also MSCs (see Suppl. Fig. S4a). The weakly negative, mostly bias- and temperature-independent (see Suppl. Note 1 and Suppl. Fig. S4f) coupling term *ECTop* is then attributed to AF coupling between two MSCs belonging to the top and central magnetic units along the nanotransport path.

The exchange-biased [15,40,43] Fe layer is magnetically hard at 17K, with $K_b \approx$ 10-20T[6] that tracks the spin-flip current (compare Figs. 2g with Suppl. Fig. S4c), while its temperature dependence (Fig. 3i) mirrors that of the exchange bias amplitude previously observed [15,40]. We find that the bottom layer's FM coupling ($J_{12}^{MSC}>0$) to the spin-flip MSC unit is primarily responsible for the latter's magnetization reversal for $|H|>1$T. This suggests that an external magnetic field may also control the transition of a MSC from an excited spin state back to its ground state. Proving this point would require carefully comparing all resistance levels (see Fig. 2f) and dI/dV (see Fig. 2g) at large *H*, when the hard bottom layer finally flips.

According to our magnetotransport model, the change in the *H* dependence of *SpinFlipMR* is associated with an abrupt decrease in J_{12}^{MSC} for T>65K (see Fig. 3h).[7] This corresponds to a E_{SF}=5.9±0.3meV magnetic anisotropy energy barrier, *i.e.* a threshold thermal energy to magnetically decouple the MSC in its excited state from the exchange-biased Fe layer and spinterface. This is consistent with the DFT-calculated ΔE=6.1meV energy difference between the MSC' ground and excited spin states when coupled to the FM.

[6] K_b is at least ≈10T in order not to witness a symmetric R(H) for V<35mV.
[7] Since the magnetization and thickness of the central unit are not well known, J_{12}^{MSC} in Tesla cannot be directly compared to the DFT's ΔE in Joule.

These results constitute direct evidence in magnetotransport of spintronic anisotropy [44,45], i.e. a change in magnetic anisotropy caused by a spin-polarized current [44,45], here due to spin excitations along MSCs. As another manifestation, while the *R(H)* loop for *V*=65mV (Fig. 2c) resembles that of *V*=80mV (Fig. 2a), maximizing the spin-flip conductance at 73meV (i.e. at the *dI/dV* peak) results in a strongly distorted *R(H)* (Fig. 2b). To the best of our knowledge, this is the first evidence of how small bias changes can so drastically alter magnetotransport. This can be modelled only through deviations in the model's parameters, especially the angle θ_{Mb} of the bottom units' anisotropy (see Suppl. Note 1).

To conclude, although a standalone chain of paramagnetic centers has no intrinsic magnetic orientation and its quantum excited states are short-lived [14], these shortcomings can be overcome by coupling [15,40,43] it to a ferromagnetic layer. We demonstrated how this enables information to be encoded in the magnetic orientation of the spin chain's excited quantum state in a solid-state device. This electrically spawned state promotes not only a change in sign of the current's spin polarization, but constitutes a distinct magnetic unit with its own coercive field. This generates a specific experimental magnetoresistance contribution against FM electrodes with a fixed spin referential. We identify the spin state by comparing its thermal stability against DFT calculations. We also use a phenomenological macrospin model of transport to pinpoint the role of magnetic coupling between the spin chain and the FM electrode in promoting this encoding capability. Our work thus implements the exchange bias concept [29] at ferromagnetic metal/molecule interfaces [15,40,43] (so-called 'spinterfaces' [31]) within the device's active spintronic layer, and articulates it with the concepts of spin-flip spectroscopy [14] and spintronic anisotropy [44,45], thanks to magnetotransport across solid-state molecular vertical

nanojunction devices. Our work thus extends prior magnetotransport research across antiferromagnetic materials [21], [22,23], [24,25] into the quantum regime.

This electrically driven MR can be used to switch the sign of MR using low-voltage addressing, and to transmit spin-wave encoded [16] information across an organic semiconducting using AF molecular spin chains in a pulsed voltage approach. Electrically controlling the quantum state of a molecular spin chain could help develop antiferromagnetic spintronics [17] at the quantum level. Our results should also stimulate the correlated oxides community to go beyond a classical picture [22,23] and exploit the quantum properties of multiferroic oxides used as the active spintronic spacer layer. Looking ahead, encoding information on this unit subsists in our work up to T≈70K. Reports [28] of intermolecular exchange coupling beyond room temperature indicate a path for applications. This can also help increase the spintronic harvesting of thermal energy fluctuation on paramagnetic centers [45].

Methods

Heterostructure stacks were grown in-situ and at room temperature in an ultra-high vacuum multichamber cluster by dc sputtering (metals) and thermal evaporation (CoPc). The SiO_x substrate was annealed at 110°C and allowed to cool down prior to deposition. After nanojunction processing (see Suppl. Note 4), the junctions were wirebonded to a sample chip and inserted onto a cryo-free magnetotransport bench. Measurements were performed in 4-point mode with (-) contacts on the lower electrode. The data acquisition time was on the order of 1s/point, with 1s between acquisitions. In the main text, the junction stack was SiO_x//Cr(5)/Fe(50)/CoPc(20)/Co(10)/Cr(5) (all numbers in nm). In addition to that junction, eight CoPc junctions with both top and bottom Fe electrodes showed MR for T<100K, five exhibited conductance increases associated with spin-flip behavior. An electrically driven MR term was observed on two junctions.

TEM characterization was performed using an aberration (image) corrected Titan 80-300 (FEI Company) operated at 300 kV and equipped with a US1000 slowscan CCD camera (Gatan Inc.). Focused ion beam (FIB) cross-sectional preparation was used for TEM sample preparation with a Strata 400-S (FEI Company). Initial cutting was performed at 30 kV followed by a fine polishing at 5 kV with a current of 47 pA and subsequently with 2 kV and a current of 28 pA. SEM imaging of the layers was minimized during the complete preparation procedure.

Supporting Information
Supporting Information is available from the Wiley Online Library or from the author.

Acknowledgements
We thank M. Gruber and Y. Henry for stimulating discussions, S. Dornier for engineering assistance, the STNano technological platform staff for technical assistance with certain processing steps, and the remaining members of the IPCMS machine shop for support. We acknowledge financial support from the Institut Carnot MICA (project 'Spinterface'), from the Region Grand Est and Synchrotron SOLEIL, from CEFIPRA grant 5604-3, from the ANR (ANR-06-NANO-033-01, ANR-09-JCJC-0137, ANR-14-CE26-0009-01), the Labex NIE "Symmix" (ANR-11-LABX-0058 NIE), the EC Sixth Framework Program (NMP3-CT-2006-033370), the Contrat de Plan Etat-Region grants in 2006 and 2008, by « NanoTérahertz », a project co-funded by the ERDF 2014-2020 in Alsace (European Union fund) and by the Region Grand Est through its FRCR call, by the impact project LUE-N4S part of the French PIA project "Lorraine Université d'Excellence", reference ANR-15IDEX-04-LUE and by the « FEDER-FSE Lorraine et Massif Vosges 2014-2020 ", a European Union Program. The calculations

were performed using HPC resources from the Strasbourg Mesocenter and from GENCI-CINES Grant gem1100.

References

[1] P. Gehring, J. M. Thijssen, and H. S. J. van der Zant, *Single-Molecule Quantum-Transport Phenomena in Break Junctions*, Nature Reviews Physics **1**, 381 (2019).
[2] J. de Bruijckere, P. Gehring, M. Palacios-Corella, M. Clemente-León, E. Coronado, J. Paaske, P. Hedegård, and H. S. J. van der Zant, *Ground-State Spin Blockade in a Single-Molecule Junction*, Physical Review Letters **122**, 197701 (2019).
[3] E. Moreno-Pineda, C. Godfrin, F. Balestro, W. Wernsdorfer, and M. Ruben, *Molecular Spin Qudits for Quantum Algorithms*, Chem. Soc. Rev. **47**, 501 (2018).
[4] K. Yoshida, I. Hamada, S. Sakata, A. Umeno, M. Tsukada, and K. Hirakawa, *Gate-Tunable Large Negative Tunnel Magnetoresistance in Ni–C $_{60}$ –Ni Single Molecule Transistors*, Nano Letters **13**, 481 (2013).
[5] N. Xin, J. Guan, C. Zhou, X. Chen, C. Gu, Y. Li, M. A. Ratner, A. Nitzan, J. F. Stoddart, and X. Guo, *Concepts in the Design and Engineering of Single-Molecule Electronic Devices*, Nature Reviews Physics **1**, 211 (2019).
[6] G. D. Scott and T.-C. Hu, *Gate-Controlled Kondo Effect in a Single-Molecule Transistor with Elliptical Ferromagnetic Leads*, Phys. Rev. B **96**, 144416 (2017).
[7] X. Chen, Y.-S. Fu, S.-H. Ji, T. Zhang, P. Cheng, X.-C. Ma, X.-L. Zou, W.-H. Duan, J.-F. Jia, and Q.-K. Xue, *Probing Superexchange Interaction in Molecular Magnets by Spin-Flip Spectroscopy and Microscopy*, Physical Review Letters **101**, 197208 (2008).
[8] M. Muenks, P. Jacobson, M. Ternes, and K. Kern, *Correlation-Driven Transport Asymmetries through Coupled Spins in a Tunnel Junction*, Nature Communications **8**, 14119 (2017).
[9] M. Ormaza, P. Abufager, B. Verlhac, N. Bachellier, M.-L. Bocquet, N. Lorente, and L. Limot, *Controlled Spin Switching in a Metallocene Molecular Junction*, Nature Communications **8**, 1974 (2017).
[10] A. Bellec, J. Lagoute, and V. Repain, *Molecular Electronics: Scanning Tunneling Microscopy and Single-Molecule Devices*, Comptes Rendus Chimie **21**, 1287 (2018).
[11] S. Karan, C. García, M. Karolak, D. Jacob, N. Lorente, and R. Berndt, *Spin Control Induced by Molecular Charging in a Transport Junction*, Nano Letters **18**, 88 (2018).
[12] S. Loth, K. von Bergmann, M. Ternes, A. F. Otte, C. P. Lutz, and A. J. Heinrich, *Controlling the State of Quantum Spins with Electric Currents*, Nat Phys **6**, 340 (2010).
[13] S. Yan, D.-J. Choi, J. A. J. Burgess, S. Rolf-Pissarczyk, and S. Loth, *Control of Quantum Magnets by Atomic Exchange Bias*, Nature Nanotechnology **10**, 40 (2015).
[14] S. Loth, C. P. Lutz, and A. J. Heinrich, *Spin-Polarized Spin Excitation Spectroscopy*, New J. Phys. **12**, 125021 (2010).
[15] M. Gruber, F. Ibrahim, S. Boukari, H. Isshiki, L. Joly, M. Peter, M. Studniarek, V. Da Costa, H. Jabbar, V. Davesne, U. Halisdemir, J. Chen, J. Arabski, E. Otero, F. Choueikani, K. Chen, P. Ohresser, W. Wulfhekel, F. Scheurer, W. Weber, M. Alouani, E. Beaurepaire, and M. Bowen, *Exchange Bias and Room-Temperature Magnetic Order in Molecular Layers*, Nat Mater. **14**, 981 (2015).
[16] J. P. Gauyacq and N. Lorente, *Excitation of Spin Waves by Tunneling Electrons in Ferromagnetic and Antiferromagnetic Spin-1/2 Heisenberg Chains*, Physical Review B **83**, (2011).
[17] V. Baltz, A. Manchon, M. Tsoi, T. Moriyama, T. Ono, and Y. Tserkovnyak, *Antiferromagnetic Spintronics*, Rev. Mod. Phys. **90**, 015005 (2018).

[18] A. A. Khajetoorians, J. Wiebe, B. Chilian, S. Lounis, S. Blügel, and R. Wiesendanger, *Atom-by-Atom Engineering and Magnetometry of Tailored Nanomagnets*, Nature Physics **8**, 497 (2012).
[19] B. Warner, F. El Hallak, H. Prüser, J. Sharp, M. Persson, A. J. Fisher, and C. F. Hirjibehedin, *Tunable Magnetoresistance in an Asymmetrically Coupled Single-Molecule Junction*, Nature Nanotechnology **10**, 259 (2015).
[20] A. D. Kent and D. C. Worledge, *A New Spin on Magnetic Memories*, Nat Nano **10**, 187 (2015).
[21] B. G. Park, J. Wunderlich, X. Martí, V. Holý, Y. Kurosaki, M. Yamada, H. Yamamoto, A. Nishide, J. Hayakawa, H. Takahashi, A. B. Shick, and T. Jungwirth, *A Spin-Valve-like Magnetoresistance of an Antiferromagnet-Based Tunnel Junction*, Nature Materials **10**, 347 (2011).
[22] Z. Sefrioui, C. Visani, M. J. Calderón, K. March, C. Carrétéro, M. Walls, A. Rivera-Calzada, C. León, R. L. Anton, T. R. Charlton, F. A. Cuellar, E. Iborra, F. Ott, D. Imhoff, L. Brey, M. Bibes, J. Santamaria, and A. Barthélémy, *All-Manganite Tunnel Junctions with Interface-Induced Barrier Magnetism*, Advanced Materials **22**, 5029 (2010).
[23] F. Y. Bruno, M. N. Grisolia, C. Visani, S. Valencia, M. Varela, R. Abrudan, J. Tornos, A. Rivera-Calzada, A. A. Ünal, S. J. Pennycook, Z. Sefrioui, C. Leon, J. E. Villegas, J. Santamaria, A. Barthélémy, and M. Bibes, *Insight into Spin Transport in Oxide Heterostructures from Interface-Resolved Magnetic Mapping*, Nature Communications **6**, 1 (2015).
[24] J. Shi, V. Lopez-Dominguez, F. Garesci, C. Wang, H. Almasi, M. Grayson, G. Finocchio, and P. Khalili Amiri, *Electrical Manipulation of the Magnetic Order in Antiferromagnetic PtMn Pillars*, Nature Electronics **3**, 92 (2020).
[25] N. L. Nair, E. Maniv, C. John, S. Doyle, J. Orenstein, and J. G. Analytis, *Electrical Switching in a Magnetically Intercalated Transition Metal Dichalcogenide*, Nature Materials **19**, 153 (2020).
[26] C. Barraud, K. Bouzehouane, C. Deranlot, S. Fusil, H. Jabbar, J. Arabski, R. Rakshit, D.-J. Kim, C. Kieber, S. Boukari, M. Bowen, E. Beaurepaire, P. Seneor, R. Mattana, and F. Petroff, *Unidirectional Spin-Dependent Molecule-Ferromagnet Hybridized States Anisotropy in Cobalt Phthalocyanine Based Magnetic Tunnel Junctions*, Phys. Rev. Lett. **114**, 206603 (2015).
[27] C. Barraud, K. Bouzehouane, C. Deranlot, D. J. Kim, R. Rakshit, S. Shi, J. Arabski, M. Bowen, E. Beaurepaire, S. Boukari, F. Petroff, P. Seneor, and R. Mattana, *Phthalocyanine Based Molecular Spintronic Devices*, Dalton Trans. **45**, 16694 (2016).
[28] M. Serri, W. Wu, L. R. Fleet, N. M. Harrison, C. F. Hirjibehedin, C. W. M. Kay, A. J. Fisher, G. Aeppli, and S. Heutz, *High-Temperature Antiferromagnetism in Molecular Semiconductor Thin Films and Nanostructures*, Nat Commun **5**, 3079 (2014).
[29] K. O'Grady, L. E. Fernandez-Outon, and G. Vallejo-Fernandez, *A New Paradigm for Exchange Bias in Polycrystalline Thin Films*, Journal of Magnetism and Magnetic Materials **322**, 883 (2010).
[30] F. Djeghloul, M. Gruber, E. Urbain, D. Xenioti, L. Joly, S. Boukari, J. Arabski, H. Bulou, F. Scheurer, F. Bertran, P. Le Fevre, A. Taleb-Ibrahimi, W. Wulfhekel, G. Garreau, S. Hajjar-Garreau, P. Wetzel, M. Alouani, E. Beaurepaire, M. Bowen, and W. Weber, *High Spin Polarization at Ferromagnetic Metal-Organic Interfaces: A Generic Property*, J. Phys. Chem. Lett. **7**, 2310 (2016).
[31] S. Delprat, M. Galbiati, S. Tatay, B. Quinard, C. Barraud, F. Petroff, Pierre Seneor, and R. Mattana, *Molecular Spintronics: The Role of Spin-Dependent Hybridization*, J. Phys. D: Appl. Phys. **51**, 473001 (2018).

[32] W. G. Wang, A. Pearse, M. Li, S. Hageman, A. X. Chen, F. Q. Zhu, and C. L. Chien, *Parallel Fabrication of Magnetic Tunnel Junction Nanopillars by Nanosphere Lithography*, Scientific Reports **3**, 1948 (2013).
[33] M. Studniarek, U. Halisdemir, F. Schleicher, B. Taudul, E. Urbain, S. Boukari, M. Hervé, C.-H. Lambert, A. Hamadeh, S. Petit-Watelot, O. Zill, D. Lacour, L. Joly, F. Scheurer, G. Schmerber, V. Da Costa, A. Dixit, P. A. Guitard, M. Acosta, F. Leduc, F. Choueikani, E. Otero, W. Wulfhekel, F. Montaigne, E. N. Monteblanco, J. Arabski, P. Ohresser, E. Beaurepaire, W. Weber, M. Alouani, M. Hehn, and M. Bowen, *Probing a Device's Active Atoms*, Advanced Materials 1606578 (2017).
[34] F. Schleicher, *Linking Electronic Transport through a Spin Crossover Thin Film to the Molecular Spin State Using X-ray Absorption Spectroscopy Operando Techniques*, ACS Appl. Mater. Interfaces **10**, 31580 (2018).
[35] S. Boukari, A. Ghaddar, Y. Henry, J. Arabski, V. Da Costa, M. Bowen, J. Le Moigne, and E. Beaurepaire, *Electrical Transport across a Structurally Ordered Phthalocyanine Film: Role of Defect States*, Physical Review B **76**, 033302 (2007).
[36] J. Tong, L. Ruan, X. Yao, G. Qin, and X. Zhang, *Defect States Dependence of Spin Transport in Iron Phthalocyanine Spin Valves*, Phys. Rev. B **99**, 054406 (2019).
[37] M. Bowen, A. Barthélémy, M. Bibes, E. Jacquet, J. P. Contour, A. Fert, D. Wortmann, and S. Blügel, *Half-Metallicity Proven Using Fully Spin-Polarized Tunnelling*, Journal of Physics: Condensed Matter **17**, L407 (2005).
[38] S. Javaid, M. Bowen, S. Boukari, L. Joly, J.-B. Beaufrand, X. Chen, Y. J. Dappe, F. Scheurer, J.-P. Kappler, J. Arabski, W. Wulfhekel, M. Alouani, and E. Beaurepaire, *Impact on Interface Spin Polarization of Molecular Bonding to Metallic Surfaces*, Physical Review Letters **105**, 077201 (2010).
[39] M. M. Deshmukh, S. Kleff, S. Guéron, E. Bonet, A. N. Pasupathy, J. von Delft, and D. C. Ralph, *Magnetic Anisotropy Variations and Nonequilibrium Tunneling in a Cobalt Nanoparticle*, Phys. Rev. Lett. **87**, 226801 (2001).
[40] S. Boukari, H. Jabbar, F. Schleicher, M. Gruber, G. Avedissian, J. Arabski, V. Da Costa, G. Schmerber, P. Rengasamy, B. Vileno, W. Weber, M. Bowen, and E. Beaurepaire, *Disentangling Magnetic Hardening and Molecular Spin Chain Contributions to Exchange Bias in Ferromagnet/Molecule Bilayers*, Nano Letters **18**, 4659 (2018).
[41] K. V. Raman, A. M. Kamerbeek, A. Mukherjee, N. Atodiresei, T. K. Sen, P. Lazić, V. Caciuc, R. Michel, D. Stalke, S. K. Mandal, S. Blügel, M. Münzenberg, and J. S. Moodera, *Interface-Engineered Templates for Molecular Spin Memory Devices*, Nature **493**, 509 (2013).
[42] W. Pan, N.-Y. Jih, C.-C. Kuo, and M.-T. Lin, *Coercivity Enhancement near Blocking Temperature in Exchange Biased Fe/FexMn1−x Films on Cu(001)*, Journal of Applied Physics **95**, 7297 (2004).
[43] S. Mallik, S. Mattauch, M. K. Dalai, T. Brückel, and S. Bedanta, *Effect of Magnetic Fullerene on Magnetization Reversal Created at the Fe/C60 Interface*, Scientific Reports **8**, 5515 (2018).
[44] M. Misiorny, M. Hell, and M. R. Wegewijs, *Spintronic Magnetic Anisotropy*, Nat Phys **9**, 801 (2013).
[45] K. Katcko, E. Urbain, B. Taudul, F. Schleicher, J. Arabski, E. Beaurepaire, B. Vileno, D. Spor, W. Weber, D. Lacour, S. Boukari, M. Hehn, M. Alouani, J. Fransson, and M. Bowen, *Spin-Driven Electrical Power Generation at Room Temperature*, Communications Physics **2**, 116 (2019).